Journal of the European Ceramic Society **16** (1996) 109–113
© 1996 Elsevier Science Limited
Printed in Great Britain. All rights reserved
0955-2219(95)00139-5
0955-2219/96/$15.00

Formation of Aluminum Rich 9:1 Mullite and its Transformation to Low Alumina Mullite upon Heating

Reinhard X. Fischer,[a]* Hartmut Schneider[b] & Dietmar Voll[b]

[a]Institut für Geowissenschaften der Universität, D-55099 Mainz, Germany
[b]German Aerospace Research Establishment (DLR), Institute for Materials Research, D-51140 Köln, Germany

(Accepted 22 July 1995)

Abstract

The formation of aluminum rich mullites $Al_{4+2x}Si_{2-2x}O_{10-x}$ *with* $x > 2/3$ *has been studied at annealing temperatures between 700 and 1650°C. Calcination of the amorphous precursor at 700°C yields a mullite with 88 mol% Al_2O_3 corresponding to an x-value of 0·809. Simultaneously, a γ-alumina phase is formed. Further increase of the annealing temperature yields an increase in the aluminum incorporation up to 92·1 mol% Al_2O_3 at 1000°C derived from the refined lattice constants. This is the highest amount of Al observed so far in a mullite except the supposed end member ι-Al_2O_3 which, however, has not yet been established unambiguously. Above 1000°C, the aluminum content in mullite is reduced. This is accompanied by a transformation of the spinel-type phase to a superstructure of a θ-alumina like phase. The final product at 1650°C consists of 34 mol% of a 'normal' mullite with* $x = 0{\cdot}32$ *and 66 mol% corundum.*

1 Introduction

An aluminum rich mullite with 89% Al_2O_3 and lattice constants $a > b$ has been described recently[1,2] and it was shown that the linear relationship between lattice constant a and the molar content of Al_2O_3 can be extrapolated beyond the crossover point of a and b lattice parameters. In the work described here we show that a sample prepared by sol–gel synthesis exhibits an even higher aluminum content at annealing temperatures below 1000°C. This sample is used to elucidate the crystallization process of mullites at the high alumina end of the solid solution series.

*Present address: Fachbereich Geowissenschaften der Universität, D-28334 Bremen, Germany.

2 Experimental

The sample was prepared as described in Refs 1 and 2. After heating at a rate of 300°C/h, the samples were kept at the respective temperatures for 15 h and subsequently quenched in air. A portion of the sample was retained for the X-ray investigations and the bulk of the sample was further heated to the next temperature step. X-ray powder diffraction data were collected with a Seifert automatic powder diffractometer with CuK_α radiation and a graphite monochromator in the diffracted beam. Samples were filled into a flat sample holder with a bottom silicon crystal to diminish background scattering. Background was subtracted by hand with a linear interpolation between consecutive breakpoints in the pattern. Phase analyses were performed by simulation of the mullite powder diagrams using the PC Rietveld plus program.[3] Calculated intensities were corrected for automatic divergence slit effects in the Rietveld procedure.[4] Data were collected in step scan mode between 10 and 100°2θ with steps of 0·03° and a counting time of 30 s per step, except for the final data set of the 1650°C sample which was measured between 5 and 140°2θ with 10 s per step.

3 Results and Discussion

Crystallization of mullite starts at about 700°C, together with the formation of a γ-alumina phase (Figs 1(a–d)). High background intensities indicate the presence of a relatively large amount of a coexisting amorphous phase. Mullite formed at 700°C exhibits broad X-ray lines of low intensity. X-ray line intensities gradually increase upon heating accompanied by a sharpening of the line widths, especially at temperatures above 900°C. This indicates an increasing degree of structural order in $a > b$ mullites heat-treated above ≈900°C.

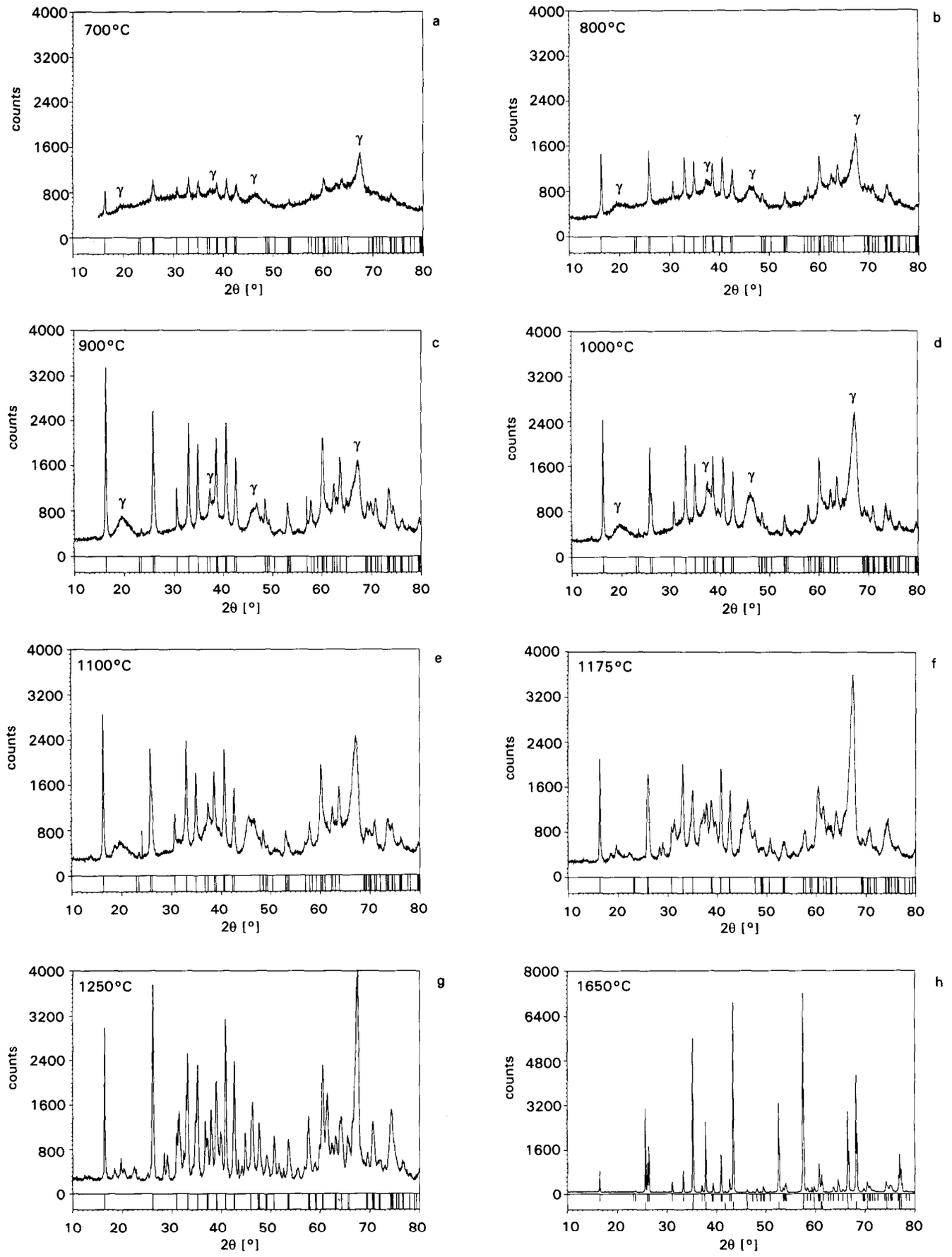

Fig. 1. Observed powder patterns of mullite samples at various annealing temperatures given in the upper left corner of the diagram frames. Mullite reflections are indicated by tickmarks underneath the powder diagrams. The broad peaks belonging to the γ-alumina phase are labeled with the Greek letter γ in Figs 1(a–d). Reflections without tickmarks in Figs 1(e–g) belong to a transformed alumina phase. Fig. 1(h) shows the powder diagrams of mullite (upper row of tickmarks) and corundum, α-alumina (bottom set of tickmarks). The sharp features at 57°2θ in Fig. 1(c) and at 24°2θ in Fig. 1(e) are spurious intensities from instrumental effects; they are eliminated in the analyses.

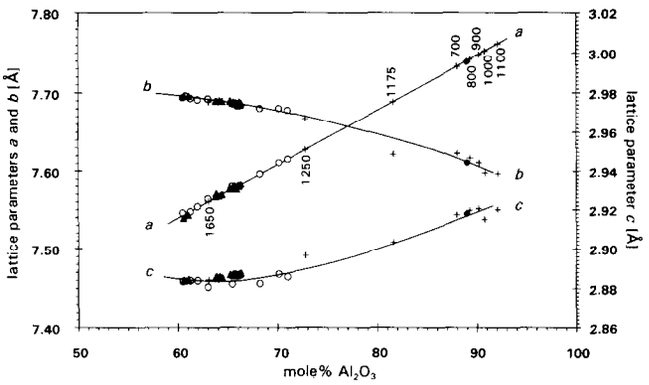

Fig. 2. Lattice parameters *a*, *b*, and *c* of mullites from recent determinations (◆ Ref. 2, ▲ Ref. 5, ○ Ref. 6) with the additional data points (+) from this work. The straight line for *a* results from linear regression, the curves for *b* and *c* are fitted by hand. Data points of this work are labeled with the respective annealing temperatures (°C).

This observation is in agreement with HRTEM studies on $a > b$ mullites prepared at 1000°C which yielded evidence for an ordered sequence of domains with high and low Oc oxygen vacancy concentrations.[5] The γ-alumina phase has the characteristic broad peaks in the powder diagram at 20, 46, and 67°2θ. Above ≈1100°C (Figs 1(e–g)), the reflections of the alumina phase become sharper. Splitting of the peaks indicates a phase transition or an ordering of the highly disordered defect spinel. At 1650°C (Fig. 1(h)), the alumina spinel phase transforms to α-alumina (corundum) and mullite exhibits very sharp diffraction peaks.

The chemical composition of the low-temperature mullites were derived from the linear relationship between its lattice constant *a* and the molar content of Al_2O_3. Using the more recent data of mullite determinations[6,7] in the low alumina region extended by the data from the high alumina mullite,[2] we get the relationships shown in Fig. 2. A linear regression based on these data (represented by the open circles, solid triangles, and the diamond symbol) yields the line drawn for lattice constant *a*. The curves for lattice constants *b* and *c* are fitted by hand. Slope *A* and intercept *B* are derived from the linear regression yielding the relation to calculate the molar content *m* of Al_2O_3 in mullite

$$a = A \cdot m + B = 0{\cdot}00692 \cdot m + 7{\cdot}124$$

and

$$m = 144{\cdot}5 \cdot a - 1029{\cdot}5$$

The uncertainties are 0·00008 for *A* and 0·005 for *B* yielding an error of about 1·5 mol% for the determination of *m* with this equation.

Lattice constants were determined by the Rietveld refining method. The accuracy of the refinements depends strongly on the accuracy of the crystal structure parameters which are used for the powder pattern simulation. Therefore, the refinement has been performed iteratively with an average structure of mullite as an initial model. This initial refinement yielded improved lattice constants which were used to redetermine the chemical composition from the curves shown in Fig. 2. The occupation factors of the Al and Si atoms were set to values derived from the *x*-values according to the formula given below (see also footnote in Table 1). This process was repeated two or three times until the best fit was achieved with the most accurate lattice constants. Regions of the spinel phase in the powder diagrams were excluded from the refinements. The resulting lattice constants, related to the molar content of Al_2O_3, can be used to derive the *x*-value in the formula of the mullite chemical composition and, consequently, the occupation factors of the respective atom sites. The *x*-value is given by

$$x = 10 - 6 \cdot \frac{m + 200}{m + 100}$$

The results are listed in Table 1. The lattice constants are added to Fig. 2 (+ symbols). While the *a* parameters inevitably lie on the straight line (since they were derived from the linear regression), the parameters *b* and *c* give a good measure for the shape of these lattice parameter curves.

Table 1. Lattice constants *a*, *b*, *c* (Å) from Rietveld refinements, molar content, *m* of Al_2O_3 (%) from linear regression, and atom site occupancies

T(°C)	*a*	*b*	*c*	*m*	*x*	*Number per unit cell*			
						Si in T	*T*,Oc**	*T***	*Oc*
700	7·7328(24)	7·6229(23)	2·9175(6)	88·0	0·809	0·383	1·191	0·426	0
800	7·7419(12)	7·6172(11)	2·9197(3)	89·3	0·830	0·340	1·170	0·489	0
900	7·7480(6)	7·6106(6)	2·9205(2)	90·2	0·845	0·311	1·155	0·534	0
1000	7·7616(9)	7·5969(8)	2·9201(2)	92·1	0·877	0·245	1·123	0·632	0
1100	7·7525(10)	7·5978(9)	2·9150(3)	90·8	0·855	0·289	1·144	0·567	0
1175	7·6889(26)	7·6222(26)	2·9034(6)	81·6	0·697	0·606	1·303	0·091	0
1250	7·6278(20)	7·6671(20)	2·8964(5)	72·8	0·528	0·944	1·056	0	0·416
1650	7·5603(3)	7·6886(3)	2·8843(1)	63·1	0·320	1·360	0·640	0	1·040

Si in T = 2–2*x*, T*,Oc*= 2–*x* for samples with $x > 2/3$ (700–1175°C) and 2*x* for samples with $x < 2/3$, T** = 3*x*–2 for samples with $x > 2/3$ else 0, Oc = 2–3*x* for samples with $x < 2/3$ else 0 (see Ref. 2 for explanation).

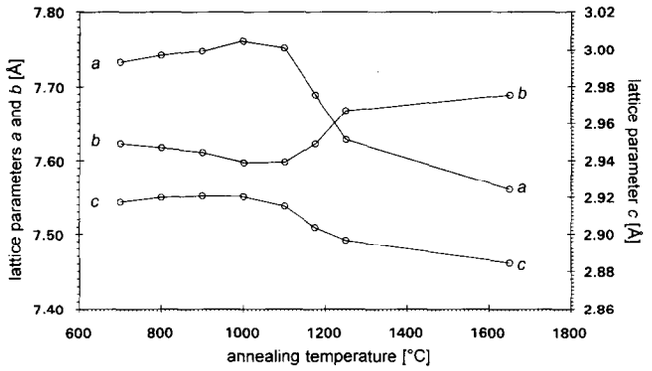

Fig. 3. Plot of lattice constants versus annealing temperature.

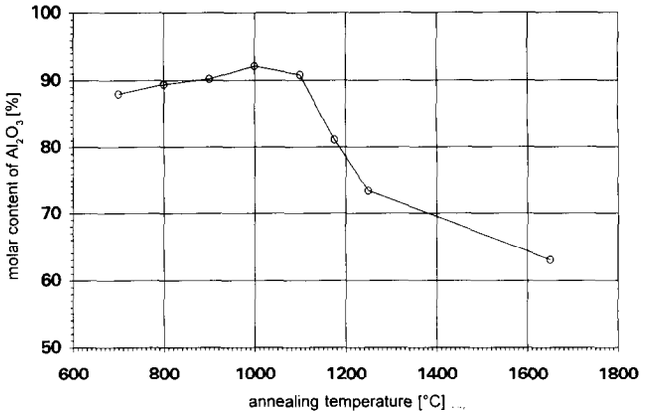

Fig. 4. Plot of molar content of Al_2O_3 versus annealing temperature.

The deviations of the parameters of the 1175 and 1250°C samples might be caused by the severe overlap of the mullite reflections with the spinel phase reflections. An improvement in the accuracy of the lattice constant determinations could be achieved by a simultaneous simulation of mullite and γ-alumina. The multiphase refinement could not be performed because of difficulties in the crystal structure determination of the spinel phase. Further work is in progress. However, the results are sufficiently accurate for a discussion of the phase formation. Figure 3 shows a plot of the lattice constants versus the annealing temperature and Fig. 4 shows the corresponding molar relationship derived from data in Fig. 2. It is notable that the lattice constant a, and consequently the molar content of Al_2O_3, increase upon heating between 700 and 1000°C. In this region, the mullite phase corresponds to the new type of mullite described in Ref. 2 (see also data in Table 1). Above 1000°C, the aluminum content is reduced, rapidly falling to values which represent a 'normal' mullite at 1250°C with lattice constants $a < b$ and with x-values $< 2/3$ corresponding to mullites with less than 80 mol% Al_2O_3. At the final temperature, at 1650°C, the sample consists of α-alumina (corundum) and a well crystallized mullite with 63% Al_2O_3. Simultaneously with the reduction in the aluminum content at 1100°C, a transformation of the spinel phase is observed indicated by the narrowing and splitting of the broad reflections at $20°2\theta$ and $46°2\theta$ (Fig. 1(e)). At 1250°C, further transformation to a θ-alumina like phase is observed with very sharp reflections indicating a well crystallized product. However, several reflections which do not fit into the monoclinic cell of θ-alumina[8] indicate a supercell with bigger lattice parameters which has not been observed before for the transition aluminas. We suspect that the reduction of the aluminum content in mullite above 1000°C is directly related to the formation of the new deformed spinel phase. Considering that the spinel phase could incorporate silicon as well[9] a discussion of the exact phase relations in this system is very difficult as long as the structure of the defect spinel has not been determined.

The final product at 1650°C contains 34 mol% mullite ($Al_{4.64}Si_{1.36}O_{9.68}$) and 66 mol% corundum ($Al_2O_3$) derived from the standardless quantitative Rietveld analysis with an absolute error of about 3%. Here, we assume that the amorphous phase completely disappeared. This corresponds roughly to a Al/Si ratio of 6:1 in the bulk composition of this sample which indicates a loss of silicon in the vigorous hydrolytic reaction of the starting materials with an initial Al/Si ratio of about 4:1.[1,2]

Acknowledgements

We thank the Deutsche Forschungsgemeinschaft (DFG) for financial support under grant Fi442/2. The award of a Heisenberg fellowship to RXF is gratefully acknowledged. We thank R. D. Shannon for reading the manuscript. Computing facilities were financially supported by the Materialwissenschaftliches Forschungszentrum of the University of Mainz.

References

1. Schneider, H., Fischer, R. X. & Voll, D., Mullite with lattice constants $a > b$. *J. Am. Ceram. Soc.*, **76** (1993) 1879–81.
2. Fischer, R. X., Schneider, H. & Schmücker, M., Crystal structure of Al-rich mullite. *Am. Mineral*, **79** (1994) 983–90.
3. Fischer, R. X., Lengauer, C., Tillmanns, E., Ensink, R. J., Reiss, C. A. & Fantner, E. J., PC-Rietveld plus, a comprehensive Rietveld analysis package for PC. *Materials Science Forum* **133–136** (1993) 287–92.
4. Fischer, R. X., Divergence slit corrections for Bragg-Brentano diffractometers with rectangular sample surface. *Powder Diffraction*, in press.
5. Schneider, H., Okada, Y., Pask, J. A., *Mullite and mullite ceramics*. Wiley & Sons, Chichester, 1994, pp. 33–4.
6. Klug, F. J., Prochazka, S. & Doremus, R. H., Alumina-silica phase diagram in the mullite region. *Ceramic Transactions*, **6** (1990) 15–43.

7. Ban, T. & Okada, K., Structure refinement of mullite by the Rietveld method and a new method for estimation of chemical composition. *J. Am Ceram. Soc*, **75** (1992) 227–30.
8. Zhou, R. -S. & Snyder, R. L., Structures and transformation mechanisms of the η, γ and θ transition aluminas. *Acta. Cryst.*, **B47** (1991) 617–30.
9. Schneider, H., Voll, D., Saruhan, B., Schmücker, M., Schaller, T. & Sebald, A., Constitution of the γ-alumina phase in chemically produced mullite precursors. *J. Europ. Ceram. Soc.*, **13** (1994) 441–8.